Study of the acoustic feedback problem of active noise control by using the l_1 and l_2 vector space optimization approaches

Mingsian R. Bai and Tianyau Wu
Department of Mechanical Engineering, Chiao-Tung University, 1001 Ta-Hsueh Road, Hsin-Chu, Taiwan, Republic of China

(Received 15 July 1996; revised 10 March 1997; accepted 8 April 1997)

This study attempts to explore the acoustic feedback problem that is frequently encountered in feedforward active noise control (ANC) structure from the standpoint of control theories. The analysis is carried out on the basis of the Youla's parametrization and the l_1-norm and l_2-norm vector space optimization. The ANC problem is formulated as a model matching procedure and is solved via linear programming in the dual vector space. These methods alleviate the problems caused by the nonminimum phase (NMP) zeros of the cancellation path. The ANC algorithms are implemented by using a digital signal processor. Various types of noises were chosen for validating the developed algorithms. The proposed methods are also compared with the well-known filtered-u least-mean square (FULMS) method. The experimental results show that the acoustic feedback problem significantly degrades the performance and stability of the ANC system regardless which method is used. Insights into the difficulties due to acoustic feedback are addressed along the line of control theories. © *1997 Acoustical Society of America.* [S0001-4966(97)03008-7]

PACS numbers: 43.50.Ki [GAD]

INTRODUCTION

The active noise control (ANC) technique has attracted much academic as well as industrial attention since it provides numerous advantages over traditional passive methods in attenuating low-frequency noises.[1,2] However, the optimistic view somewhat masks the complexity of many theoretical and technical problems that remain to be solved prior to full commercialization of the technique. Among the difficulties, the acoustic feedback problem of the feedforward structure has been the plaguing issue that seriously impedes successful application of the ANC technique. This problem usually arises in a feedforward ANC structure that is generally the only practical approach for suppressing broadband random noises, where in many practical situations only the upstream acoustical reference is available. In this configuration, a positive feedback loop will exist between the canceling loudspeaker and the feedforward microphone, which tends to destabilize the ANC system. Consider the ANC system for a duct shown in Fig. 1. Suppose that only the noise below the cutoff frequency of the duct is of interest so that the control problem can be treated as a one-dimensional problem. The secondary loudspeaker generates a canceling sound to interact destructively with the primary noise field. It is desired that the noise will be attenuated as much as possible at the error microphone position. It is further assumed that only the acoustical reference at the upstream of the canceling source is available, as usually is the case in practical applications. Unfortunately, the canceling loudspeaker on a duct wall will generate plane waves propagating both upstream and downstream. Therefore, the antisound output to the loudspeaker not only cancels noise downstream by minimizing the error signals measured by the error microphone but also radiates upstream to the reference microphone, resulting in a corrupted reference signal. The coupling of the acoustic wave from the canceling loudspeaker to the reference microphone is called *acoustic feedback*.[3] Similar effects take place in the active vibration control system due to feedback from the control actuator to the reference sensor. Because the upstream feedforward microphone will detect both the noise from the primary source and the noise produced by the canceling loudspeaker, the positive acoustic feedback problem can no longer be ignored. It is this positive feedback problem that seriously complicates the active control design.

The fact that acoustic feedback introduces poles to the system and thus a stability problem if the loop gain becomes too large has been illustrated by Eghtesadi and Leventhall.[1,4] Another good review concerning acoustic feedback can be found in Chapter 3 of the book by Kuo and Morgan.[3] The solutions to the problem of acoustic feedback cited in the book included directional microphones and loudspeakers, motional feedback loudspeakers, neutralization filter, dual-microphone reference sensing, the filter-u least-mean square (FULMS) method, nonacoustic sensors, and so forth.

This paper adopts a new approach to explore the acoustic feedback problem in the ANC application domain from the standpoint of control theories. The analysis is carried out on the basis of the Youla's parametrization[5] and the l_1-norm and l_2-norm vector space optimization.[6] The performance of the developed methods is compared with the well-known FULMS algorithm that has long been recognized as one of the elegant solutions to the acoustic feedback problem.[3,7] The simplicity of the proposed methods stems from the fact that the ANC problem is formulated as a model matching procedure and is solved via linear programming (LP) in the dual vector space. These methods optimally tackle the problem of unstable inverse resulting from the inherent nonminimum phase (NMP) property of the cancellation path (which frequently occurs to structural systems or acoustical systems).

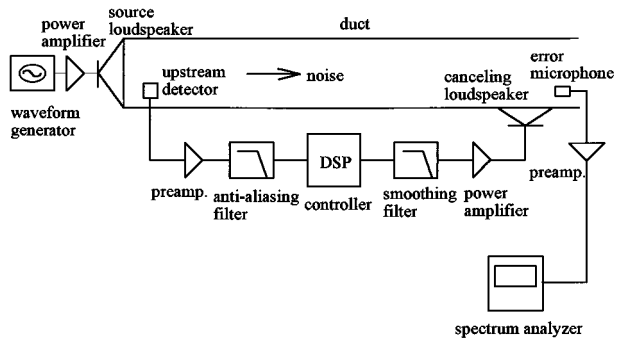

FIG. 1. Schematic diagram of the feedforward ANC structure for a duct in the presence of acoustic feedback.

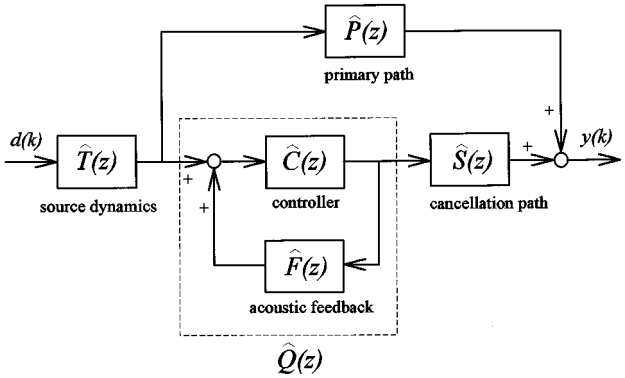

FIG. 2. System block diagram of the feedforward ANC structure in the presence of acoustical feedback. $\hat{P}(z)$, $\hat{S}(z)$, $\hat{F}(z)$, and $\hat{C}(z)$ are the discrete time transfer functions of the primary path, the cancellation path, the acoustic feedback path, and the controller, respectively.

The l_1 and l_2 ANC algorithms are implemented by using a floating-point digital signal processor. Various types of noises including white noise, engine exhaust noise, and sweep sine were chosen for validating the developed algorithms. It will be seen from the experimental results that the acoustic feedback problem indeed significantly degrades the performance and stability of the ANC system regardless of which ANC method is used. Additional insights into the difficulties due to acoustic feedback are also addressed in this paper within a general framework of control theories.

I. THE l_1 AND l_2 ANC ALGORITHMS

The l_1 control theory emerged in the 1980s. Dahleh and Pearson proposed an l_1 compensator to track persistent bounded signals.[8] The same authors also applied the l_1 control theory to reject bounded persistent disturbances by solving a semi-infinite LP problem.[9] Deodhare and Vidyasagar performed an in-depth analysis of the condition of when a stabilizing controller is l_1 optimal.[10] An excellent review of the l_1 control theory can be found in the text by Dahleh and Diaz-Bobillo.[6] In the sequel, the l_1 control theory is only presented in the context of the ANC problem.

As mentioned previously, the acoustic feedback problem is very detrimental in terms of performance and stability of the ANC system. In what follows, the analysis of acoustic feedback problem in the ANC application domain is carried out from the standpoint of control theories. To begin with, the ANC problem is formulated as a model matching problem,[11] as shown in the block diagram of Fig. 2. The sampled signal $d(k)$ is the input disturbance noise and $y(k)$ is the residual field detected at the error microphone position. The primary path, $\hat{P}(z)$, is the transfer function formed by the primary acoustic path, the power amplifier, the upstream sensor, and the error microphone, where z denotes the z transform variable. $\hat{S}(z)$ is the transfer function of the cancellation path formed by the canceling loudspeaker, the power amplifier, the secondary acoustic path, and the error microphone. $\hat{F}(z)$ is the transfer function of the acoustic feedback path formed by the canceling loudspeaker, the power amplifier, the acoustic path, and the upstream sensor. The transfer function $\hat{C}(z)$ represents the controller to be designed. In particular, $\hat{T}(z)$ is a transfer function describing the source dynamics formed by the primary source, a power amplifier, an acoustical path, and the upstream microphone. Hence, the feedforward ANC problem in the presence of acoustical feedback amounts to finding the controller $\hat{C}(z)$ such that the residual field $y(k)$ can be minimized. This is a generic model matching problem. That is,

$$\min_{C(z)} \left\| T(z)\left[P(z)+S(z)\,\frac{C(z)}{1-F(z)C(z)}\right]\right\|, \tag{1}$$

where $\|(.)\|$ is the notation of function norm. Note that the transfer function, $\hat{T}(z)$, can be regarded as a weighting function for the terms inside the parenthesis. In practice, $\hat{T}(z)$ may not be measurable so that either analytical modeling or heuristic guess is needed.

By Youla's parametrization, the controller $\hat{C}(z)$ that guarantees the internal stability of the closed loop system can be expressed as[12]

$$\hat{C}(z)=\frac{\hat{M}(z)\hat{Q}(z)+\hat{Y}(z)}{\hat{N}(z)\hat{Q}(z)+\hat{X}(z)}, \tag{2}$$

where $\hat{Q}(z)$ is a stable, proper, and real-rational function [denoted as $\hat{Q}(z)\in RH^{\infty}$],[12] $\hat{F}(z)=\hat{N}(z)/\hat{M}(z)$ is the coprime factorization of $\hat{F}(z)$, and $\hat{X}(z)\in RH^{\infty}$ and $\hat{Y}(z)\in RH^{\infty}$ satisfy the Bezout identity[12]

$$\hat{M}(z)\hat{X}(z)-\hat{N}(z)\hat{Y}(z)=1. \tag{3}$$

If the plant is proper and stable, as it is in our case, one may simply let[12] $\hat{M}(z)=1$, $\hat{N}(z)=\hat{F}(z)$, $\hat{X}(z)=1$, and $\hat{Y}(z)=0$. Then the controller in Eq. (2) turns out to be

$$\hat{C}(z)=\frac{\hat{Q}(z)}{\hat{F}(z)\hat{Q}(z)+1}. \tag{4}$$

Substituting Eq. (4) into Eq. (1) leads to

$$\min_{Q(z)\in RH^{\infty}} \|T(z)[P(z)+S(z)Q(z)]\|. \tag{5}$$

It is noteworthy that the model matching problem in Eq. (5) is exactly of the same form as that of the purely feedforward ANC system (in the absence of acoustic feedback) by replacing the designed controller $\hat{C}$ by a parameter $\hat{Q}$ that is indicated by the dashed line in Fig. 2. Since $\hat{S}(z)$ is usually

NMP, it is desirable to develop an algorithm that would effectively match the primary path and the cancellation path with respect to some optimal criterion, especially when the NMP behavior is present. Elegant solutions to this problem are available in the robust control theory. Two model matching algorithms capable of dealing with NMP problems in ANC applications are presented in this paper. The optimal solution of Eq. (5), $\hat{Q}_{\text{opt}}(z)$, can be found by either l_1 or l_2 optimization procedure.

$$\min_{Q\in l_1}\|P+S*Q\|_1=\min_{H\in l_1}\|G+H\|_1$$

or (6)

$$\min_{Q\in l_2}\|P+S*Q\|_2=\min_{H\in l_2}\|G+H\|_2,$$

where P and S are pulse response sequences of the primary path and the cancellation path, respectively, ''*'' represents convolution, $G=P$, $H=S*Q$, ''$\|\cdot\|_{1,2}$'' denotes the 1-norm or 2-norm, and l_1 denotes the normed linear space of all bounded sequences with bounded 1-norm.[13]

The following derivation contains a fair amount of mathematical definitions and results. However, the l_1 theories are quite standard in functional analysis[14] and vector space optimization,[13] and we present only the key ones needed in the development of the l_1-ANC algorithm. The rest are mentioned without proof.

The minimum distance problem in the primal space posed in Eqs. (6) can be recast into a maximum problem in its dual space. Let X be a normed linear space; f is said to be a bounded linear functional on X if f is a continuous linear operator from X to $\Re$. A dual space of X, denoted by X^*, is the collection of all bounded linear functionals on X, equipped with the natural induced norm. Whenever f is represented by some element $x^*\in X^*$, we use the notation $\langle x,x^*\rangle$ to represent the value $f(x)$. Then, a vector is said to be *aligned* with its normed dual if the following relation is satisfied[13]

$$\langle x,x^*\rangle=\|x^*\|\|x\|. \tag{7}$$

Given a sequence $h=[h(1)\ h(2)\ h(3)\ \cdots]'$ in l_1, where the prime denotes matrix transpose, we also need the definition of λ transform of h to facilitate the following derivations of l_1 algorithm.

$$\hat{H}(\lambda)=\sum_{k=0}^{\infty}h(k)\lambda^k. \tag{8}$$

Unlike the Z transform, it should be noted that the λ transform is defined in terms of an infinite series of positive powers. It is obvious that $\hat{H}(\lambda)$ is BIBO (bounded-input–bounded-output, i.e., both the input and the output are l_∞ sequences) stable if and only if h is an l_1 sequence.[8] In addition, the space c_0 is defined as the space of all infinite sequences in l_∞ of real numbers converging to zero.

With the aforementioned definitions, we are in a position to find the optimal solution of the model matching problem in Eqs. (6). Assume that $\hat{S}(\lambda)$ has no zeros on the unit circle. Then the so-called *interpolation constraints* must be satisfied.[8] Let $\hat{S}(\lambda)$ have N NMP zeros denoted by a_i, $i=1,2,\cdots,N$, and $|a_i|<1$, each of multiplicity γ_i, then

$$\hat{H}^{(k)}(a_i)=0,\quad i=1,2,\ldots,N;\quad k=0,1,\ldots,\gamma_i-1, \tag{9}$$

where the superscript (k) denotes the kth derivative of a complex function. The key of the solution to the optimization problem in Eqs. (6) is based on the following *duality theorem*.[15]

Theorem: Given the system of m consistent linear equations in n unknowns $Ax=y$, then

$$\min_{Ax=y}\|x\|_p=\max_{\|A'u\|_q\leqslant 1}(y'u), \tag{10}$$

where $1/p+1/q=1$, $1<p,\ q<\infty$. Furthermore, optimal x and $A'u$ are aligned. According to the theorem, the primal problem (which is a minimization problem) can be converted to a maximization problem in its dual space. By the duality theorem, it can be shown that the l_1 optimization problem in Eq. (6) becomes[6]

$$d_{\text{opt}}=\|\phi_{\text{opt}}\|_1=\min_{V_\infty'\phi=\Gamma}\|G+H\|_1=\max_{\|V_\infty x\|_\infty\leqslant 1}(\Gamma'x), \tag{11}$$

where d_{opt} is the minimal distance, $\phi=G+H=[\alpha_1\ \alpha_2\ \alpha_3\cdots]'$ is the error vector, ϕ_{opt} is the optimal ϕ,

$$\Gamma=[\hat{G}(a_1)\hat{G}^{(1)}(a_1)\cdots\hat{G}^{(\gamma_1)}(a_1)\hat{G}(a_2)\times\hat{G}^{(1)}(a_2)\cdots\hat{G}^{(\gamma_2)}(a_2)\cdots\hat{G}^{(\gamma_N)}(a_N)]',\ x\in\Re^m,$$

and

$$V_\infty=\begin{bmatrix}\text{Re}(a_1^0) & \ldots & \text{Re}(a_N^0) & \text{Im}(a_1^0) & \ldots & \text{Im}(a_N^0)\\ \text{Re}(a_1^1) & \ldots & \text{Re}(a_N^1) & \text{Im}(a_1^1) & \ldots & \text{Im}(a_N^1)\\ \vdots & & \vdots & \vdots & & \vdots\end{bmatrix}.$$

In the matrix V_∞, Re.$(\cdot)$ and Im$(\cdot)$ denote the real part and the imaginary part, respectively. Note also that the interpolation constraints in Eq. (9) has been rewritten as $V_\infty'\phi=\Gamma$. Hence the infinite-dimensional optimization problem has become a finite-dimensional one. The only pitfall is that the LP problem in Eq. (11) has infinitely many constraints. However, because $|a_i|<1$, it can be shown that only a finite number of these constraints are really necessary.[6] More precisely, we can compute an integer, L, such that any α_i satisfies the first L constraints also satisfies the remaining ones. Define a real Vandermonde matrix of order L

$$V_L=\begin{bmatrix}\text{Re}(a_1^0) & \ldots & \text{Re}(a_N^0) & \text{Im}(a_1^0) & \ldots & \text{Im}(a_N^0)\\ \text{Re}(a_1^1) & \ldots & \text{Re}(a_N^1) & \text{Im}(a_1^1) & \ldots & \text{Im}(a_N^1)\\ \vdots & & \vdots & \vdots & & \vdots\\ \text{Re}(a_1^L) & \ldots & \text{Re}(a_N^L) & \text{Im}(a_1^L) & \ldots & \text{Im}(a_N^L)\end{bmatrix}. \tag{12}$$

Hence, the matrix V_∞ in Eq. (11) can everywhere be replaced by V_L. If a_i is real, then the column of zeros corresponding to the imaginary part is dropped. If a_i is complex, either a_i or its complex conjugate $\overline{a_i}$ is considered. Note that the matrix V_L has full column rank for all $L\geqslant 2N$. An upper bound on

the number of the constraints, $L(\geqslant 2N)$, can be computed *a priori*:[6]

$$\max_i |a_i|^L (L|V_L^{-l}|_1) < 1, \quad i = 1,2,\ldots,N, \tag{13}$$

where V_L^{-l} is the left inverse of V_L.

The beauty of the above l_1 approach lies in the fact the infinite-dimensional model matching problem in Eq. (11) has been converted to a standard LP problem described by

$$d_{\text{opt}} = \max_{\|V_L x\| \leqslant 1} (\Gamma' x), \tag{14}$$

which can be conveniently solved in the dual space by using an LP routine. Then the corresponding optimal solution is recovered in the primal space via the alignment conditions. Define

$$\phi_{L,\text{opt}} = [\alpha_1 \quad \alpha_2 \quad \cdots \quad \alpha_L]' \in l_1$$

and

$$b = [\beta_1 \quad \beta_2 \quad \cdots \quad \beta_L]' = V_L x_{\text{opt}} \in \mathscr{C}_0.$$

The l_1 version of the alignment conditions are stated as:[6,15] (a) $\alpha_i = 0$ if $|\beta_i| < 1$; (b) $\alpha_i \beta_i \geqslant 0$ if $|\beta_i| = 1$. However, only part (a) of the alignment conditions in conjunction with the interpolation constraints, $V_L' \phi = \Gamma$, are needed for determining the components of $\phi_{L,\text{opt}}$. After $\phi_{L,\text{opt}}$ has been solved, the finite-impulse response function $\hat{\phi}_{L,\text{opt}}(z)$ can be expressed (by using the fact $\lambda = z^{-1}$) as

$$\hat{\phi}_{L,\text{opt}}(z) = \alpha_1 + \alpha_2 z^{-1} + \cdots + \alpha_L z^{-(L-1)}. \tag{15}$$

By the same token, the feedforward ANC problem can be formulated as an l_2 model matching problem. The minimization problem in the primal space can be converted to a maximization problem in the dual space by the duality theorem:

$$\begin{aligned} d_{\text{opt}} &= \|\phi_{L,\text{opt}}\|_2 = \min_{\mathbf{V}_{L^*}' \Phi = \Gamma} \|G - H\|_2 = \max_{\|\mathbf{V}_{L^*} \mathbf{x}\|_2 \leqslant 1} [\Gamma' \mathbf{x}], \\ \Gamma &= [\hat{G}(a_1)\hat{G}^{(1)}(a_1)\cdots\hat{G}^{(\gamma_1)}(a_1)\hat{G}(a_2) \\ &\quad \times \hat{G}^{(1)}(a_2)\cdots\hat{G}^{(\gamma_2)}(a_2)\cdots\hat{G}^{(\gamma_N)}(a_N)]', \end{aligned} \tag{16}$$

where the notations are the same as those defined in Eq. (11). It can be shown that the alignment condition leads directly to the optimal solution[5,14]

$$\phi_{L,\text{opt}} = V_L (V_L' V_L)^{-1} \Gamma \tag{17}$$

with the corresponding minimum distance

$$d_{\text{opt}} = [\Gamma' (V_L' V_L)^{-1} \Gamma]^{1/2}. \tag{18}$$

Note that the inverse of $(V_L' V_L)$ is guaranteed since V_L is of full column rank. The only difference between the l_2 optimization and the l_1 optimization is that the former does not require explicit solution of the dual problem.

Next, both the l_1 and l_2 optimal parameters, $\hat{Q}_{\text{opt}}(z)$, can be obtained by backsubstituting $\hat{\phi}_{L,\text{opt}}(z)$ into Eq. (11) or Eq. (16) as follows:

$$\hat{Q}_{\text{opt}}(z) = [\hat{\phi}_{L,\text{opt}}(z) - \hat{P}(z)]/\hat{S}(z). \tag{19}$$

It should be noted that, because the interpolation constraints have been satisfied, the NMP zeros of $\hat{S}(z)$ will always be canceled by $\hat{\phi}_{L,\text{opt}}(z) - \hat{P}(z)$ to ensure the stability of the parameter $\hat{Q}_{\text{opt}}(z)$. After $\hat{Q}_{\text{opt}}(z)$ is obtained, the optimal controller $\hat{C}_{\text{opt}}(z)$ can be recovered by the following formula:

$$\hat{C}_{\text{opt}}(z) = \frac{\hat{Q}_{\text{opt}}(z)}{\hat{F}(z)\hat{Q}_{\text{opt}}(z) + 1}. \tag{20}$$

A note regarding the implementation of the above l_1 controller and l_2 controller is in order. In some cases, it may occur that these methods result in controllers with excessive gains in the high-frequency range. This is due to the fact that the control algorithms attempt to compensate for the NMP zeros in high frequencies that may be only artificially created from discretization.[16] To alleviate the problem, remedies may be sought by incorporating a small constant ϵ into $\hat{S}(z)$, i.e.,

$$S(z) \rightarrow [S(z) + \epsilon] \tag{21}$$

so that the plant is not excessively rolled off.

In some cases, the resulting controller $\hat{C}_{\text{opt}}(z)$ can be unstable, even though the parameter $\hat{Q}_{\text{opt}}(z)$ is guaranteed to be proper and stable. This fact has been illustrated in an acoustic analysis in frequency domain of a simplified infinite-length duct model detailed in the paper by Eghtesadi and Leventhall.[4] An alternative argument from the viewpoint of control theory will lead to similar observation as follows. Let the transfer function between the disturbance $d(k)$ and the residual output $y(k)$ be $\hat{P}_1(z)$. Recall that $d(k)$ is assumed to be inaccessible and only $\hat{P}(z) = \hat{P}_1(z)\hat{T}^{-1}(z)$ is subject to some sort of experimental system identification procedure. However, it happens more often than never that the system, $\hat{T}(z)$, is NMP such that $\hat{T}(z)$ has no stable inverse. Direct identification of the plant $\hat{P}(z)$ generally results in unstable or nearly unstable systems, even though both $\hat{P}_1(z)$ and $\hat{T}(z)$ are stable. Hence, it is likely that the identified $\hat{P}_1(z)$ involves large modeling error and the best one can get is only an approximation of the inherently unstable $\hat{T}^{-1}(z)$. This approximation further degrades the performance of active control in comparison with the purely feedforward structure. Nevertheless, this modeling difficulty can be alleviated somewhat by appropriate introduction of passive damping. The importance of passive damping treatment that has often been overlooked in active design lies in not only high-frequency attenuation but also the robustness of active control with respect to plant uncertainties.[17] Another benefit of using passive damping is that lower order of plant models can usually be obtained than the lightly damped plants so that numerical error is reduced.

II. EXPERIMENTAL RESULTS

Experiments were conducted to validate the adaptive l_1 and l_2 ANC algorithms. A rectangular duct of length 1 m and cross section $0.25\ \text{m} \times 0.25\ \text{m}$ was chosen for this test. The duct is lined with fiberglass sound-absorbing material to create sufficient acoustical damping that is crucial to the ro-

TABLE I. The poles and zeros of the primary path $\hat{P}(z)$, the cancellation path $\hat{S}(z)$, and the acoustic feedback path $\hat{F}(z)$.

$\hat{P}(z)$		$\hat{S}(z)$		$\hat{F}(z)$	
Zeros	Poles	Zeros	Poles	Zeros	Poles
9.9496	−0.9028±	0	0.9603±	0	−0.7521±
−1.7015	0.1998*i*	0	0.1314*i*	0	0.4749*i*
−0.9043	−0.9801	0	0.7822±	0	−0.8119±
−0.9067±	−0.8536	−13.9155	0.4891*i*	2.0484±	0.2015*i*
0.1871*i*	−0.7881±	1.0253	0.4660±	1.8137*i*	−0.4763±
−0.7956±	0.3770*i*	0.9604	0.7756*i*	−1.0837±	0.7045*i*
0.3710*i*	−0.7128±	0.6763±	0.5821±	2.0421*i*	−0.3262±
−0.7101±	0.5819*i*	0.6445*i*	0.5469*i*	1.0389	0.7085*i*
0.5863*i*	−0.5956±	0.3838±	0.1132±	0.9233	−0.0983±
−0.5852±	0.6923*i*	0.7692*i*	0.8661*i*	0.6327±	0.8864*i*
0.7100*i*	−0.4439±	0.1332±	−0.9756	0.6693*i*	0.3223±
−0.4414±	0.7825*i*	0.8898*i*	−0.2417±	0.3143±	0.8489*i*
0.7944*i*	−0.3999±	−0.2228±	0.8059*i*	0.7870*i*	0.2237±
−0.3101±	0.7295*i*	0.7830*i*	−0.7367±	−1.0706	0.7123*i*
0.8503*i*	−0.2992±	−0.7419±	0.3400*i*	−0.8401±	0.6590±
−0.1585±	0.8666*i*	0.2637*i*	−0.5724±	0.3254*i*	0.6588*i*
0.9111*i*	−0.1497±	0.5260±	0.5447*i*	−0.0532±	−0.7800±
0.0666±	0.9207*i*	0.4643*i*	−0.3582±	0.7865*i*	0.4911*i*
0.9405*i*	0.0704±	0.4790	0.6160*i*	−0.4994±	0.8501±
0.2757±	0.9221*i*	−0.5067	0.6335	0.4428*i*	0.2237*i*
0.8730*i*	0.9975			−0.2340±	0.9579±
0.5087±	0.8880±			0.6325*i*	0.1476*i*
0.8030*i*	0.2575*i*				−0.7250
0.6232±	0.8813±				
0.7250*i*	0.3695*i*				
1.0075	0.7996±				
0.8902±	0.4107*i*				
0.2599*i*					
0.7559±	0.7463±				
0.5024*i*	0.5074*i*				
0.8051±	0.6792±				
0.4125*i*	0.6363*i*				
0.5630±	0.2653±				
0.1642*i*	0.8560*i*				
	0.5036±				
	0.7872*i*				
	0.4152±				
	0.6802*i*				
delay=3,	gain=−0.0247	delay=0,	gain=0.0720	delay=1,	gain=0.0064

bustness of the ANC system, as has been mentioned previously. The corresponding cutoff frequency of the duct is 690 Hz and thus only plane waves are of interest. The controller was implemented by using a floating-point TMS320C31 digital signal processor. The sampling frequency was chosen to be 2 kHz. Fourth-order Butterworth filters with cutoff frequency 600 Hz were used as the anti-aliasing filter and the smoothing filter. The experimental setup including the duct, the upstream sensor, the error microphone, the actuator, the controller, and signal conditioning circuits has been shown in Fig. 1. The ARX system identification procedure[18] was used for establishing the mathematical models of the primary path, the cancellation path, and acoustic feedback path whose poles and zeros are listed in Table I. The frequency response functions of the primary path, the cancellation path, and the acoustic feedback path are shown in Figs. 3–5. The frequency response function of the chosen weighting function in Eq. (5) is shown in Fig. 6. The frequency response

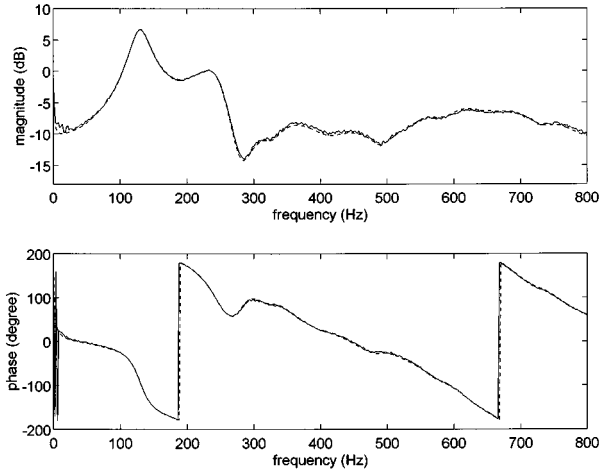

FIG. 3. The frequency response function of the primary path $\hat{P}(z)$. Measured data: ———; model data: -----.

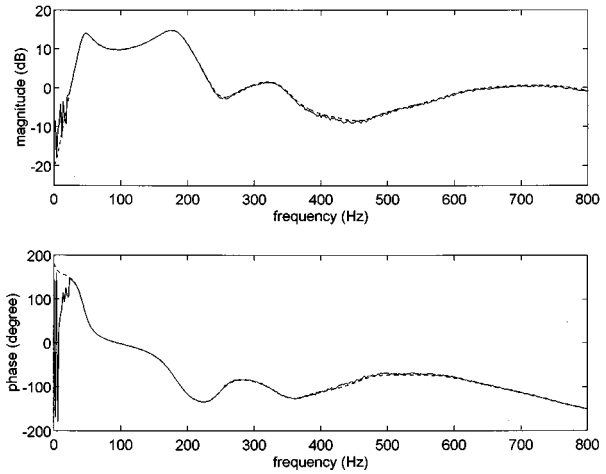

FIG. 4. The frequency response function of the cancellation path $\hat{S}(z)$. Measured data: ———; model data: -----.

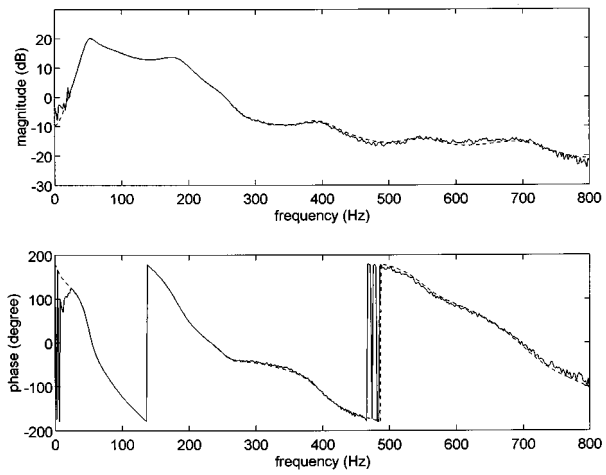

FIG. 5. The frequency response function of the acoustic feedback path plant $\hat{F}(z)$. Measured data: ———; model data: -----.

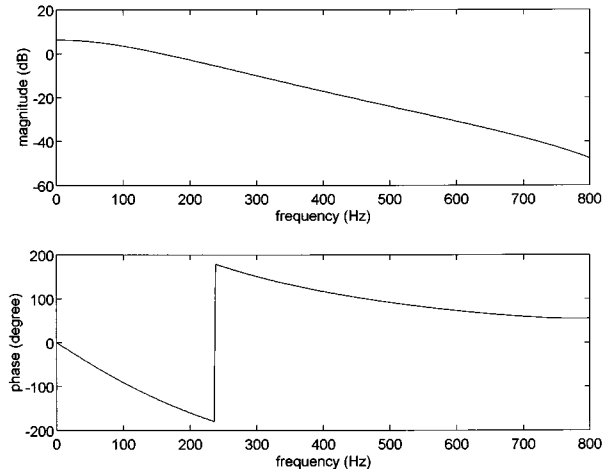

FIG. 6. The frequency response function of the chosen weighting function $\hat{T}(z)$ in Eq. (5).

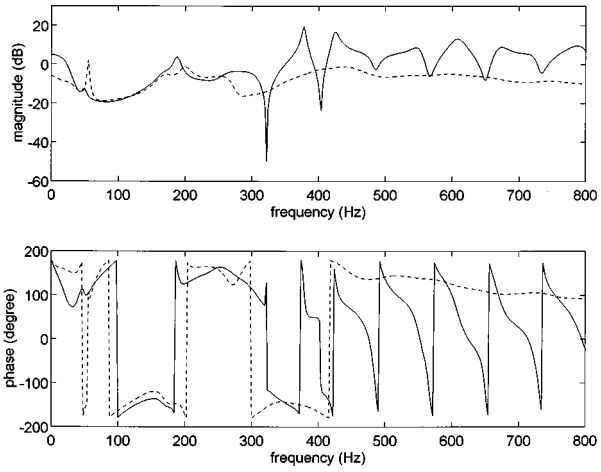

FIG. 7. The frequency response functions of the l_1 and l_2 controllers in the experimental cases of Table II. l_1 controller: ———; l_2 controller: -----.

functions of the optimal controllers designed by the aforementioned l_1 and l_2 procedure are then shown in Fig. 7.

To compare the performance of the ANC techniques, three types of noises including a white noise, a sweep sine, an engine exhaust noise were employed as the primary noises. The experimental cases and the associated noise types and control algorithms are summarized in Table II.

Case 1 is a reference case of purely feedforward l_1 control, where the source voltage signal is used as the feedforward reference so that acoustic feedback can be neglected. It can be seen from the result of Fig. 8 that significant attenuation (approximately 5–20 dB) is obtained in the frequency range 60–330 Hz. In cases 2–4, the signal detected by an upstream microphone is used as the feedforward reference so that the effect of acoustic feedback is present. In these cases, the widely used FULMS algorithm, the l_1 algorithm, and the l_2 algorithm are employed for attenuating the white noise. The power spectra of the residual fields at the error microphone position with and without active control are shown in Figs. 9, 10, and 11 for cases 2, 3, and 4, respectively. Attenuation (approximately 3–20 dB) was obtained from the FULMS method in the frequency range 50–200 Hz. The result was obtained 1 min after the active control was activated. However, in Fig. 9, a strong peak was found at 235 Hz in the spectrum with the FULMS algorithm. On the other hand, attenuation (approximately 2–30 dB) was obtained from the l_1 and l_2 method in the frequency range 50–220 Hz. Total attenuation within the dominant band 0–400 Hz is found to be 1.96 dB, 2.31 dB, and 2.93 dB for the FULMS method, the l_1 method, and the l_2 method, respectively. Although the total attenuation appears to be comparable, these three control algorithms give different emphasis for different frequency ranges. The FULMS method produced most attenuation (approximately 20 dB) around 100 Hz, whereas the l_1 and l_2 methods produced most attenuation (approximately 30 dB) around 200 Hz. The FULMS method is prone to have a stability problem, as compared with the l_1 method, and the

TABLE II. Experimental case design.

Case	Noise type	Algorithm	Tap/step[a]	Figure
1[b]	white noise	l_1	···	8
2	white noise	FULMS	30/0.0001	9
3	white noise	l_1	···	10
4	white noise	l_2	···	11
5	sweep sine	FULMS	30/0.0001	12
6	sweep sine	l_1	···	13
7	engine exhaust noise	FULMS	30/0.0001	14
8	engine exhaust noise	l_1	···	15

[a]''Tap/step'' denotes the tap length and the step size used in the FULMS algorithm.
[b]Case 1 is a reference case of purely feedforward control.

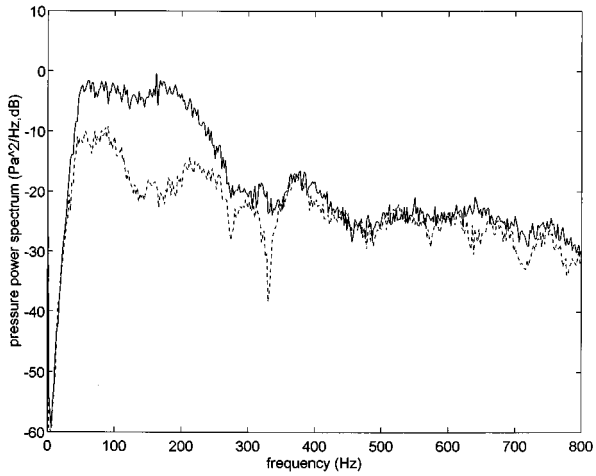

FIG. 8. The residual sound-pressure spectra of case 1 for the white noise in the absence of acoustic feedback before and after ANC is activated by using the purely feedforward l_1 controller. Control off: ———; control on: -----.

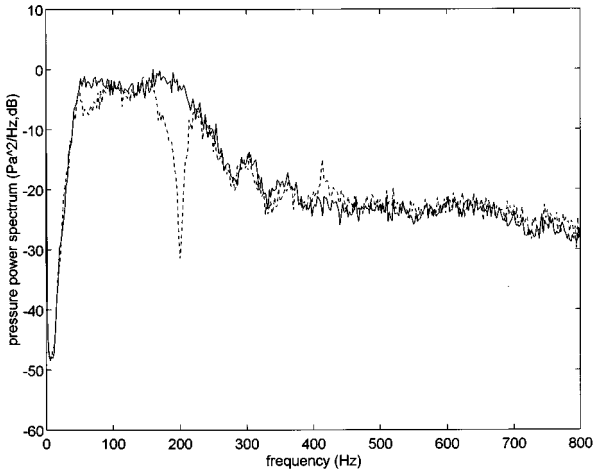

FIG. 10. The residual sound-pressure spectra of case 3 for the white noise in the presence of acoustic feedback before and after ANC is activated by using the l_1 controller. Control off: ———; control on: -----.

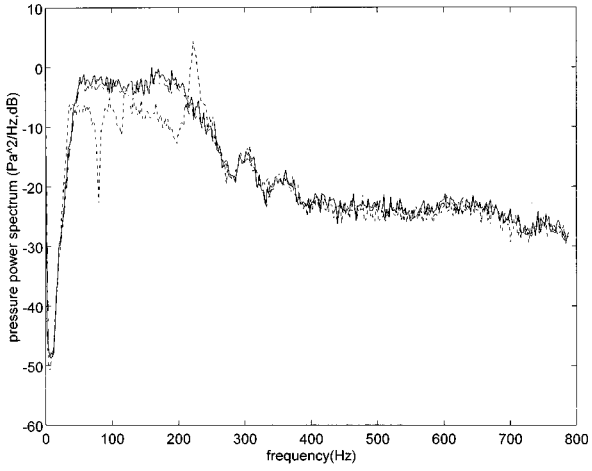

FIG. 9. The residual sound-pressure spectra of case 2 for the white noise in the presence of acoustic feedback before and after ANC is activated by using the FULMS and FXLMS controllers. The step sizes in FULMS and FXLMS are both 0.0001. The filter length in FULMS and FXLMS are 30 and 128, respectively. Control off: ———; FULMS: ---; FXLMS: –·–·.

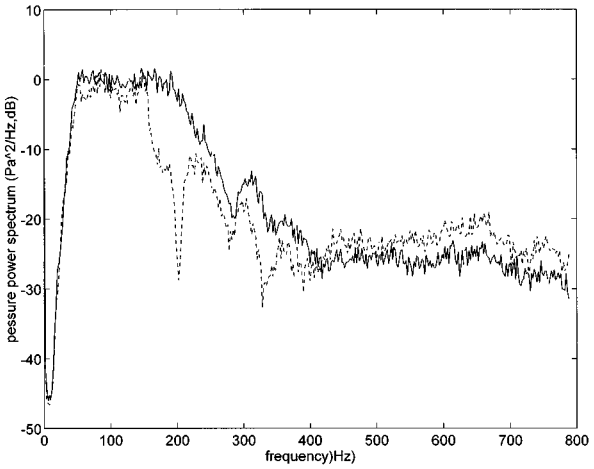

FIG. 11. The residual sound-pressure spectra of case 4 for the white noise in the presence of acoustic feedback before and after ANC is activated by using the l_2 controller. Control off: ———; control on: -----.

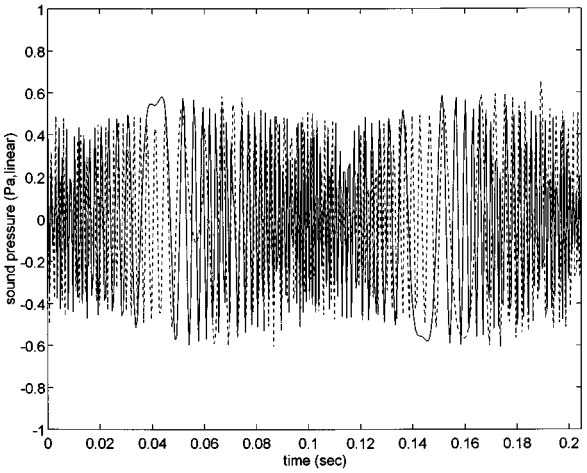

FIG. 12. The time-domain response of case 5 for the sweep sine in the presence of acoustic feedback before and after ANC is activated by using the FULMS controller. The step size in FULMS is 0.0001. The filter length is 30. Control off: ———; control on: -----.

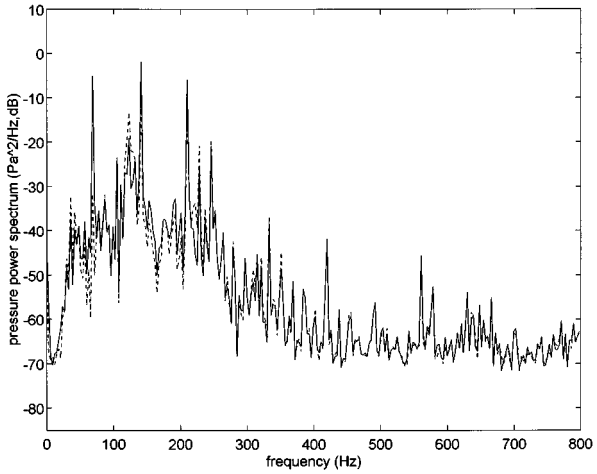

FIG. 14. The residual sound-pressure spectra of case 7 for the engine exhaust noise in the presence of acoustic feedback before and after ANC is activated by using the FULMS controller. The step size in FULMS is 0.0001. The filter length is 30. Control off: ———; control on: -----.

control drifts away slowly so that the system may become unstable. This is probably because the performance index of the FULMS algorithm is not quadratic and the computation is easily trapped in local minima. In any rate, the detrimental effect of acoustic feedback is evidenced from these results. Regardless of which method is used, the performance of noise attenuation is significantly degraded in comparison with the purely feedforward control in case 1. For the sake of comparison, the filtered-x least-mean square (FXLMS) method that is known to be effective for the purely ANC problems without acoustic feedback is also employed to tackle the same case. The result of Fig. 9 shows virtually no cancellation for the method. This is not totally unexpected since the optimal solution of the adaptive filter is generally an IIR function with poles and zeros when acoustic feedback is present.[3] This rational function can only be approximated by an FIR function of infinitely long order. In practice, finite order of the FIR filter has to be used in conjunction with a very small step size for stability reasons. This results in extremely slow convergence in real applications. In the following cases, the results of FXLMS is thus omitted for brevity.

In contrast to cases 2–4 that deal mainly with stationary noises, a sweeping sinusoidal noise is chosen in cases 5 and 6 to compare the effectiveness of the FULMS method and the l_1 method in suppressing a nonstationary noise. The time-domain results of Figs. 12 and 13 show that the l_1 method gives better performance than the FULMS method. This result is expected since the l_1 controller is essentially a fixed controller that does not require adaptation time like the FULMS controller.

In cases 7 and 8, a practical noise, the engine exhaust noise, is employed as the primary noise for comparing the FULMS method and the l_1 method. The power spectra of the residual fields at the error microphone position with and without active control are shown in Figs. 14 and 15. The result of the FULMS method was obtained 1 min after the active control was activated. Total attenuation within the dominant band 0–500 Hz is found to be 6.65 dB and 2.73 dB

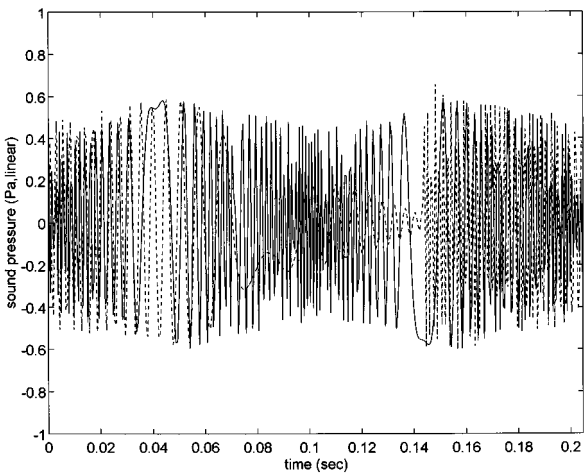

FIG. 13. The time-domain response of case 6 for the sweep sine in the presence of acoustic feedback before and after ANC is activated by using the l_1 controller. Control off: ———; control on: -----.

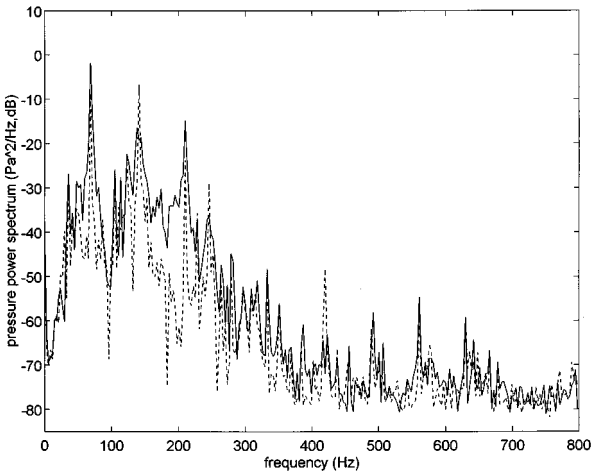

FIG. 15. The residual sound-pressure spectra of case 8 for the engine exhaust noise in the presence of acoustic feedback before and after ANC is activated by using the l_1 controller. Control off: ———; control on: -----.

for the FULMS method and the fixed l_1 method, respectively. Although cases 5–8 contain only the results of the FULMS method and the fixed l_1 method, the l_2 method yields similar performance as the l_1 method and the corresponding results are omitted for brevity.

III. CONCLUSION

Acoustic feedback problem of the feedforward ANC structure is explored from the standpoint of control theories. Feedforward ANC systems based on l_1 and l_2 model matching algorithms have been implemented by using a digital signal processor with acoustical feedback taken into account. The ANC algorithms are derived by using the Youla's parametrization and the l_1-norm and l_2-norm vector space optimization. These methods alleviate the problems caused by the nonminimum phase (NMP) zeros of the cancellation path. Passive damping treatment was introduced to improve the robustness of the control design. It is found from the theoretical and experimental investigations that the acoustic feedback significantly complicates the control design and degrades the performance and stability of the active control system because of the modeling error involved in approximating the inverse source dynamics.

The performance of the l_1 and l_2 techniques was compared experimentally with the well-known FULMS method in the presence of acoustic feedback for three kinds of noise. Although in some cases the total attenuation appears to be comparable, these active control algorithms provide different emphasis for different frequency ranges. The experimental investigations indicate the proposed methods have potential in suppressing not only stationary noises but also transient noises, where in the latter case the FULMS algorithm is generally ineffective. This is not to mention the problem of stability and local minima with the FULMS algorithm. That makes the proposed ANC systems attractive alternative for dealing with acoustic feedback problem in industrial applications.

Despite the preliminary success, the performance of the ANC system is seriously limited by the undesirable acoustic feedback regardless of which method is used. In addition, the proposed controller is fixed in nature whose practicality will be limited in the face of system perturbations. Possibilities of different acoustic arrangements, different ANC structures with more number of transducers that are unaffected by acoustic feedback, and an adaptive version of the l_1/l_2 controller will be explored in the future study.

ACKNOWLEDGMENTS

This paper was written in memory of late Professor Anna M. Pate, Iowa State University. Special thanks also go to Professor J. S. Hu for the helpful discussions on the l_1 model matching principle. The work was supported by the National Science Council in Taiwan, Republic of China, under the Project No. NSC 83-0401-E-009-024.

[1] P. A. Nelson and S. J. Elliott, *Active Control of Sound* (Academic, New York, 1992).
[2] C. R. Fuller and A. H. von Flotow, ''Active control of sound and vibration,'' IEEE Control Systems Magazine, 9–19 (December 1995).
[3] S. M. Kuo and D. R. Morgan, *Active Noise Control Systems: Algorithms and DSP Implementations* (Wiley, New York, 1995).
[4] K. H. Eghtesadi and H. G. Leventhall, ''Active attenuation of noise. The monopole system,'' J. Acoust. Soc. Am. **71**, 608–611 (1982).
[5] D. C. Youla, H. A. Jabr, and J. J. Bongiorno, Jr., ''Modern Wiener–Hopf design of optimal controllers, Part II: The multivariable case,'' IEEE Trans. Autom. Control **AC-21**, 319–338 (1976).
[6] M. A. Dahleh and J. Diaz-Bobillo, *Control of Uncertain Systems* (Prentice-Hall, Englewood Cliffs, NJ, 1995).
[7] L. J. Eriksson, ''Development of the filtered-u algorithm for active noise control,'' J. Acoust. Soc. Am. **89**, 257–265 (1990).
[8] M. A. Dahleh and J. B. Pearson, ''l_1-optimal feedback controllers for MIMO discrete-time systems,'' IEEE Trans. Autom. Control **AC-32**, 314–322 (1987).
[9] M. A. Dahleh and J. B. Pearson, ''Optimal rejection of persistent disturbances, robust stability, and mixed sensitivity minimization,'' IEEE Trans. Autom. Control **33**, 722–731 (1988).
[10] G. Deodhare and M. Vidyasagar, ''l_1-optimality of feedback control systems: The SISO discrete-time case,'' IEEE Trans. Autom. Control **35**, 1082–1085 (1990).
[11] T. C. Tsao, ''Optimal feedforward digital tracking controller design,'' ASME J. Dynam. Syst. Measurement Control **116**, 583–592 (1994).
[12] J. C. Doyle, B. A. Francis, and A. R. Tannenbaum, *Feedback Control Theory* (Maxwell Macmillan, New York, 1992).
[13] D. G. Luenberger, *Optimization by Vector Space Methods* (Wiley, New York, 1969).
[14] W. Rudin, *Functional Analysis* (McGraw-Hill, New York, 1973).
[15] J. A. Cadzow, ''Functional analysis and the optimal control of linear discrete systems,'' Int. J. Control **17**, 481–495 (1973).
[16] K. J. Astrom, P. Hagander, and J. Sternby, ''Zeros of sampled systems,'' Automatica **20**, 31–38 (1984).
[17] R. Gueler, A. H. von Flotow, and D. W. Vos, ''Passive damping for robust feedback control of flexible structure,'' AIAA J. Guid. Control Dynam. **16**, 662–667 (1993).
[18] L. Ljung, *System Identification: Theory for the User* (Prentice-Hall, Englewood Cliffs, NJ, 1987).